

Computer Simulation of Communication in Bacterial Populations under External Impact of Signal-Degrading Enzymes * **

Christina Kuttler¹[0000-0002-5521-4159] and
Anna Maslovskaya²[0000-0002-5628-3519]

¹ Technical University of Munich, Munich, Germany
kuttler@ma.tum.de

² Amur State University, Blagoveshchensk, Russia
maslovskaya@mail.ru

Abstract. Time-dependent reaction-diffusion models of cell-to-cell bacterial communication in Gram-negative bacteria are developed with a focus on the application of numerical methods and computer simulation techniques. To model bacterial communication process in the special case of quorum sensing, we consider an initial-boundary value problem for a semilinear reaction-diffusion system. To solve the problem numerically, we propose a computational algorithm based on a finite difference approach and Monte-Carlo simulations of bacterial population dynamics. A special application software is designed in Matlab to perform computer simulations of time-dependent characteristics of bacterial cooperative behavior. The computer-simulated characteristics providing quorum sensing are presented in the context of their changes under the external addition of the defined signal and enzyme. The results of the computational experiments are discussed in view of the importance of controlling the bacterial quorum sensing by means of the artificial impact of natural enzymes.

Keywords: Bacterial communication · Quorum sensing · Reaction-diffusion model · Finite difference method · Iterative algorithm · Monte-Carlo simulation · Computer-animated signal substances.

1 Introduction

At the present stage, the design and development of mathematical models describing reaction-diffusion systems in biology and medicine have both, fundamental scientific and practical interest. Among the most relevant applied problems, one can single out a class of models of microbiological communities, in particular,

* Supported by the German Academic Exchange Service (DAAD), funding programm number 57507437

** Copyright ©2020 for this paper by its authors. Use permitted under Creative Commons License Attribution 4.0 International (CC BY 4.0).

the model of the cell-to-cell communication of bacterial colonies due to quorum sensing. In biology, quorum sensing describes ability of bacteria to detect and respond to the (local) cell population density by a process of signaling and gene regulation [16, 17]. This phenomenon is attributed to producing diffusible signaling compounds by bacterial cells. The quorum sensing results in variability and (often) mutual communication of bacteria. A bacterial colony with a high local density can activate a variety of cellular processes including cooperative activities, resistance to antibiotics and virulence factors [18].

The application of mathematical modelling and computer simulation techniques to study bacterial cooperative behaviour is very useful for predicting and controlling responses of bacterial communities to external exposures. It is less costly and less time-consuming than laboratory experiments and allows even the analysis of situations which may be not accessible by wet experiments, in case of the system is already well-known. The mechanism of the bacterial quorum sensing has been previously formalized mathematically as a dynamic system described by ordinary differential equations [2, 11]. Numerous studies based on a variety of model modifications have been reported elsewhere, taking into account bacterial population growth, feedback processes in formation of signal compounds, a delay effect in a biological system, killing bacteria by antibiotics, etc. [11, 13, 14]. In addition, the description of heterogeneous space distributions of bacterial quorum sensing signaling molecules has been proposed in the form of a system of reaction-diffusion parabolic partial differential equations (PDEs) [7]. This model is most suitable for specific bacterial strains which can produce special enzymes (in particular, Lactonase), degrading signal substances produced by bacteria. Such an inhibition of quorum sensing is also called "quorum quenching" [1, 4].

The strength of intercellular communication can be potentially reduced by chemical agents. In these terms specific enzymes are promising candidates used for degrading signaling molecules. Disconnected bacteria create biofilms with essential difficulties, making them more vulnerable to both the immune system and antimicrobial drugs. Biological studies have indicated that natural enzymes can be used as inhibitors to prevent the development of infections caused by pathogens [1]. Moreover, the idea of creating alternative antibiotics related to the concept of natural enzymes application is under investigations [12].

In addition, the process of bacterial cell-to-cell communications under non-equilibrium conditions by supplying external signal substances has been the focus of intense research efforts, e.g., [3, 9]. In contrast to the previous case, the addition of signalling compounds can lead to an amplification of the signal and increasing bacterial community activities due to the positive feedback and the other nonlinear interactions. But it may also lead to a faster decrease of the signal, e.g., in the case of *P. putida* which produces the signal-degrading Lactonase in a quorum sensing controlled way. As for some pathogenic bacterial species their pathogeneity is controlled by quorum sensing, quorum quenching processes are under discussion as possible treatments [4]. Therefore, it would be of special interest to model the behaviour of time-dependent characteristics of

quorum sensing taking into account the external addition of Lactonase or other similar enzymes.

The current study aims at the further development of the dynamic semi-linear reaction-diffusion model of bacterial quorum sensing with a focus on the application of numerical methods and computer simulation techniques. The contributions of this work are presented as follows: the computational approach for modelling bacterial quorum sensing based on an iterative finite difference scheme and a Monte-Carlo simulation of bacterial population growth, and the dynamic characteristics of the biological system estimated by computational experiments under the conditions of artificial additions of signal and/or enzymes.

2 Problem Formulation

2.1 Quorum Sensing: A Concise Biological Setup

In order to introduce the main characteristics of the state of a dynamic system, let us present a brief formalized description of the bacterial communication process due to quorum sensing, without pretending to be a complete exposition of the biological foundations of this multifaceted and complex phenomenon. To be definite, we will assume that the class of Gram-negative bacteria is under consideration. More concretely, we survey a class of *Pseudomonas* bacterial species, namely, *Pseudomonas putida* IsoF (*P. putida*). This bacterial strain is one of the most studied from the point of view of the observation of joint dynamic processes: the quorum sensing and quorum quenching by an enzymatic activity.

The functional regulation network of the quorum sensing mechanism in *P. putida* is shown in Fig. 1.

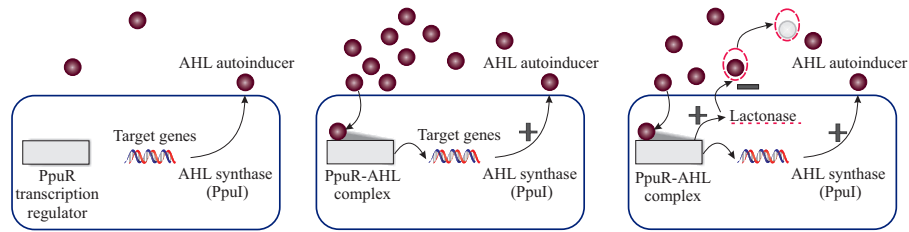


Fig. 1. Sketch of the sequential stages of the quorum sensing regulatory network in *P. putida* (Ppu).

Bacterial quorum-sensing is realized by the generation and distribution of special signaling molecules or autoinducers (N-acyl Homoserine Lactones – the short notation AHL will be used hereinafter), which allows the bacterial colony to control its behaviour by gene regulation dependent on the local population density and to form a response to external influences. The other elements of the regulation system are the follows: The AHL synthases are enzymes responsible

for the synthesis of autoinducers (proteins of the LuxI family), and transcriptional regulators, which play important role in coordinating the expression of a variety of genes (proteins of the LuxR family). The AHL can penetrate through cell membranes (out and in), then diffuses. Inside the cells, it stimulates regulatory proteins. This process results in increasing the AHL concentration as a function of the cell density due to a positive feedback in the biological regulation system.

For special bacterial strains like *P. putida* IsoF, specific self-produced Lactonase enzymes can degrade AHL-autoinducers. The generation of Lactonase can be associated with the appearance of negative feedback in a dynamic system. Also, during the evolution of the bacterial population, the natural degradation of the AHL and Lactonase occur.

The systematical approach allows us to arrive at a mathematical model of bacterial quorum sensing, which can be expressed by a system of time-dependent reaction-diffusion equations [7].

2.2 Dynamic Reaction-Diffusion Model of Quorum Sensing

The system of the following time-varying semilinear reaction-diffusion PDEs describes the dynamic biological system in the spatially one-dimensional case:

$$\frac{\partial U}{\partial t} = D_U \frac{\partial^2 U}{\partial x^2} - \gamma_U U - \gamma_{L \rightarrow U} L U + F_1(x, U), \quad (1)$$

$$\frac{\partial L}{\partial t} = D_L \frac{\partial^2 L}{\partial x^2} - \gamma_L L + F_2(x, U), \quad 0 < x < l, \quad 0 < t \leq T, \quad (2)$$

where $U(x, t)$ is the AHL concentration and $L(x, t)$ the Lactonase concentration produced by bacteria in mol/l; l is the linear size of the domain solution in μm ; T is the observation time in h.

The model parameters will be specified in the following section devoted to computational experiments. The governing equations (1), (2) define the dynamics and diffusion of AHL and Lactonase concentrations, the natural degradation of AHL and Lactonase, the production of AHL (positive feedback), the production of the Lactonase and the degradation of AHL by Lactonase (negative feedback).

We consider V discrete bacterial colonies. The source functions $F_1(x, U)$ and $F_2(x, U)$ are specified using the normal distribution of bacterial cells density and the general form of the Hill function:

$$F_m(x, U) = \sum_{v=1}^V f_m \exp\left(-\frac{(x - x_c^v)^2}{\sigma^2}\right), \quad m = 1, 2, \quad (3)$$

$$f_1(U) = \alpha_U + \beta_U \frac{U^n}{((U_{th})^n + U^n)}, \quad f_2(U) = \beta_L \frac{U^n}{((U_{th} + \varepsilon)^n + U^n)}, \quad (4)$$

where x_c^v is the position of the bacterial colony with $v = 1, \dots, V$; σ , ε , α_U , β_U , β_L , U_{th} , n are model parameters which also should be specified.

The equations (1), (2) are completed with an appropriate set of initial and boundary conditions:

$$U(x, 0) = 0, \quad L(x, 0) = 0, \quad 0 \leq x \leq l, \quad (5)$$

$$U(0, t) = 0, \quad U(l, t) = 0, \quad L(0, t) = 0, \quad L(l, t) = 0, \quad 0 \leq t \leq T. \quad (6)$$

We can stress that the basic model of quorum sensing (1)–(6) can be extended by introducing the two-dimensional analogue. In this case we use a 2D solution domain and define the dependent variables as functions $U(x, y, t)$ and $L(x, y, t)$ for the AHL concentration and Lactonase concentrations. Here the diffusion terms are written in the form $U_{xx} + U_{yy}$ and $L_{xx} + L_{yy}$, respectively. Corresponding transformations of the functions (3), (4), initial and boundary conditions (5), (6), should be performed related to the two-dimensional case.

Thus, the mathematical model is formalized by the initial-boundary value problem for system of semilinear reaction-diffusion PDEs (1)–(6). Some aspects concerning existence and uniqueness of solutions can be found in [7]. The current study focuses on the application of numerical methods, namely finite difference methods combined with a Monte-Carlo simulation, to find an adequate solution of the problem (1)–(6).

3 Numerical Aspects of the Computational Algorithm

3.1 Finite Difference Iterative Scheme for One-dimensional Problem

The initial-boundary value problem (1)–(6) was solved numerically by an implicit three-layer difference method combined with an iterative procedure [15]. Let us introduce a rectangular space-time grid covering a solution domain:

$$\Omega_h^T = \{x_i = (i - 1)h, \quad i = 1, 2, \dots, N + 1, \quad t^k = (k - 1)\tau, \quad k = 1, 2, \dots, K + 1\},$$

where N and K are the positive integers.

The model equations (1) and (2) can be rewritten in the following general view, that can be suitably used for modeling both AHL as well as Lactonase concentrations:

$$\frac{\partial v}{\partial t} = D \frac{\partial^2 v}{\partial x^2} - wv + F, \quad (7)$$

where $w = \gamma_U + \gamma_{L \rightarrow U} L$ for the equation (1) and $w = \gamma_L$ for the equation (2).

So far as we have a nonlinear term in (7), the iterative sequence $\{v_i^{(s)}\}$ for $s = 1, 2, \dots$ for each time layer $k + 1$ is derived, converging to v_i^{k+1} . As an initial approximation for the iterative sequence, we take for each $k + 1$ time layer $v_i^{(1)} = v_i^k$. Here we use the Crank–Nicolson scheme to find a solution at the second time layer. After some transformations, we get for $i = 2, 3, \dots, N$, $s = 1, 2, \dots$, taking into account the initial conditions:

$$\left[-\frac{D\tau}{2h^2} \right] v_{i-1}^{(s+1)} + \left[1 + \frac{D\tau}{h^2} + \frac{\tau}{2} w_i^2 \right] v_i^{(s+1)} + \left[-\frac{D\tau}{2h^2} \right] v_{i+1}^{(s+1)} = \frac{\tau}{2} \left(\tilde{F} + F(x_i, 0) \right), \quad (8)$$

where $\tilde{F} = F(x_i, U_i^{(s)})$ is the source function for the equation (1) and $\tilde{F} = F(x_i, 0)$ is the source function for the equation (2).

For others nodes we apply the three-layer implicit finite-difference scheme [15]. This yields that for $i = 2, 3, \dots, N$, $k = 2, 3, \dots, K$, $s = 1, 2, 3, \dots$ we arrive at

$$\begin{aligned} \left[-\frac{2D\tau}{h^2}\right] v_{i-1}^{(s+1)} + \left[3 + \frac{4D\tau}{h^2} + 2\tau w_i^{k+1}\right] v_i^{(s+1)} + \left[-\frac{2D\tau}{h^2}\right] v_{i+1}^{(s+1)} = \\ = 4v_i^k - v_i^{k-1} + 2\tau\tilde{F}, \end{aligned} \quad (9)$$

where $w_i^{k+1} = \gamma_L$ for the equation (2) and $w_i^{k+1} = \gamma_U + \gamma_{L \rightarrow U} L_i^{k+1}$ for the equation (1), $\tilde{F} = F(x_i, U_i^{(s)})$ for the equation (1) and $\tilde{F} = F(x_i, U_i^k)$ for the equation (2).

A standard procedure of approximation analysis for the computational scheme (8), (9) results in the second order accuracy with respect to space and time variables, $O(h^2 + \tau^2)$. However, to estimate the Lactonase concentration, we use of the value of the AHL concentration from the previous time layer k . This can lead to reducing the accuracy of the general scheme. To avoid this problem numerically, we apply a procedure based on a predictor-corrector approach. Actually, first, we solve the equation for the Lactonase concentration, then we calculate the AHL concentration, and finally using the specified value for the AHL concentration on the $k + 1$ time layer, we estimate the refined value for the Lactonase concentration applying the same schemes (8), (9) with $\tilde{F} = F(x_i, U_i^{k+1})$.

The initial and boundary conditions are also satisfied: $v_1^k = 0$, $v_{N+1}^k = 0$ for $k = 1, 2, \dots, K + 1$, $v_i^1 = 0$ for $i = 1, 2, \dots, N + 1$. In many practical situations, the use of iterative procedures in solving semilinear reaction-diffusion equations allows one to keep the level of accuracy corresponding to the order of approximation of the applied numerical method [5, 6, 8]. Also, the stability analysis by the linear approximation leads to absolute stability as well as unconditional monotony of the numerical scheme (9). The system of linear algebraic equations is solved efficiently by the high accuracy sweep method on each time layer.

3.2 Finite Difference Iterative Scheme for the Two-Dimensional Problem

Similarly, the two-dimensional model equations can be attributed to the general form of

$$\frac{\partial v}{\partial t} = D \left(\frac{\partial^2 v}{\partial x^2} + \frac{\partial^2 v}{\partial y^2} \right) - wv + F. \quad (10)$$

In this case we assume Ω_{h_1, h_2}^τ to be a space-time grid covering a solution domain: $\Omega_{h_1, h_2}^\tau = \{x_i = (i - 1)h_1, i = 1, 2, \dots, N + 1, y_j = (j - 1)h_2, j = 1, 2, \dots, M + 1, t^k = (k - 1)\tau, k = 1, 2, \dots, K + 1\}$. To solve the equation (10), here we apply a splitting finite-difference method, namely the alternating direction method [15]. At the first semi-step $k + 1/2$ for $i = 2, 3, \dots, N$, $j = 1, 2, \dots, M$,

$k = 1, 2, \dots, K$, $s = 1, 2, \dots$ we can define:

$$\begin{aligned} & \left[-\frac{D\tau}{2h_1^2} \right] v_{i-1,j}^{(s+1)} + \left[1 + \frac{D\tau}{h_1^2} + \frac{\tau w_{i,j}^{k+1/2}}{2} \right] v_{i,j}^{(s+1)} + \left[-\frac{D\tau}{h_1^2} \right] v_{i+1,j}^{(s+1)} = \\ & = v_{i,j}^k + \frac{D\tau}{2h_2^2} [v_{i,j-1}^k - 2v_{i,j}^k + v_{i,j+1}^k] + \frac{\tau}{2} \tilde{F}, \end{aligned} \quad (11)$$

where for the $k + 1/2$ time layer the iterative sequence $\{v_{i,j}^{(s)}\}$ converges to the value $v_{i,j}^{k+1/2}$, starting with $v_{i,j}^{(1)} = v_{i,j}^k$; $w_{i,j}^{k+1/2} = \gamma_L$ for the equation (2) and $w_{i,j}^{k+1/2} = \gamma_U + \gamma_{L \rightarrow U} L_{i,j}^{k+1/2}$ for the equation (1).

We define $\tilde{F} = F(x_i, y_j, U_{i,j}^k)$ for the equation (2) (to estimate the Lactonase concentration), then we use $\tilde{F} = F(x_i, y_j, U_{i,j}^{(s)})$ for the equation (1) for the AHL concentration, and then, again calculate the Lactonase concentration using $\tilde{F} = F(x_i, y_j, U_{i,j}^{k+1/2})$. Further we derive the scheme for the second time semistep $k + 1$:

$$\begin{aligned} & \left[-\frac{D\tau}{2h_2^2} \right] v_{i,j-1}^{(s+1)} + \left[1 + \frac{D\tau}{h_2^2} + \frac{\tau w_{i,j}^{(s+1)}}{2} \right] v_{i,j}^{(s+1)} + \left[-\frac{D\tau}{h_2^2} \right] v_{i,j+1}^{(s+1)} = \\ & = v_{i,j}^{k+1/2} + \frac{D\tau}{2h_1^2} [v_{i-1,j}^{k+1/2} - 2v_{i,j}^{k+1/2} + v_{i+1,j}^{k+1/2}] + \frac{\tau}{2} \tilde{F}, \end{aligned} \quad (12)$$

where the iterative sequence $\{v_{i,j}^{(s)}\}$ converges to the $v_{i,j}^{k+1}$, starting with $v_{i,j}^{(1)} = v_{i,j}^{k+1/2}$, $w_{i,j}^{k+1} = \gamma_L$ for the equation (2) and $w_{i,j}^{k+1} = \gamma_U + \gamma_{L \rightarrow U} L_{i,j}^{k+1}$ for the equation (1); $\tilde{F} = F(x_i, y_j, U_{i,j}^{k+1/2})$ is defined for the equation (2), $\tilde{F} = F(x_i, y_j, U_{i,j}^{(s)})$ – for the equation (1).

Here, we apply the similar approach to estimate source functions. The equations (11) and (12) are also complemented by the discrete initial and boundary conditions: $v_{i,j}^1 = 0$ for $i = 1, 2, \dots, N + 1$, $j = 1, 2, \dots, M + 1$, $v_{1,j}^k = 0$, $v_{N+1,j}^k = 0$ for $j = 1, 2, \dots, M + 1$, $k = 1, 2, \dots, K + 1$, and $v_{i,1}^k = 0$, $v_{i,M+1}^k = 0$ for $i = 1, 2, \dots, N + 1$, $k = 1, 2, \dots, K + 1$.

The derived scheme has the second order of approximation with respect to space and time variables $O(h_1^2 + h_2^2 + \tau^2)$. Likewise to the one-dimensional case, we can apply the sweep method to solve the obtained system on each time semistep.

3.3 Stochastic Algorithm for the Bacterial Population Dynamics

Evidently, the model with static positions and sizes of bacterial colonies does not suitable describe a realistic behaviour of microbe populations and, as a consequence, spatial distributions of signal compounds. In this case we combine the

quorum sensing model with the time-dependent simulation of bacterial nucleation and growth. During this process, a “mother” bacterial cell enlarges and divides into two new “daughter” cells and these new bacterial cells can also nucleate later. In general, the growth of bacterial population is a complex process, which has geometrical, exponential or logistical character. Here we use the ideas of stochastic principles of bacterial nucleation and the logistic mechanism of bacterial growth. Thus, we combine the deterministic approach for the AHL and Lactonase concentrations with a stochastic procedure to describe changes in positions of bacterial colonies.

The stochastic algorithm includes the following steps. First, up to three bacterial colonies with different probabilities start to grow simultaneously from randomly chosen points (for example, x_c^v for the one-dimensional case) as shown in Fig. 2. All bacterial colonies are assumed to grow with a similar velocity. The value of the linear size $R^v(t)$ of each bacterial colony is determined by the logistic law of growth. According to the Monte-Carlo method, a new bacterial “nucleus” can appear at a fixed random time moment, but with a small probability on each time layer. Then a new colony begins to grow in a self-similar way also according to the logistic law. If the cells are overlapping, the source functions F_1 and F_2 are determined by a superposition of colonies contributions.

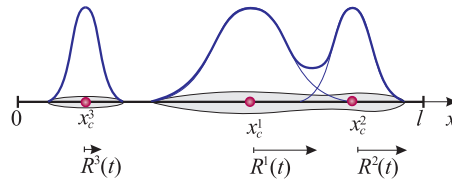


Fig. 2. The example of a state of bacterial population during growth phase.

The general computational schemes both for 1D model and 2D model were implemented in Matlab. The designed application software can be used to perform computer simulations of time-dependent characteristics of bacterial cooperative behaviour at given parameters.

4 Computer Simulations Results and Discussion

In order to perform computer simulation we need to specify the conditions of model implementation and initialize model parameters. For instance, let us take a set of parameters estimated for the bacterial strain *P. putida* IsoF (see Table 1), which have been reported previously in [7].

We aim to observe the simulation process during the defined time period varied over the range 10-30 h. For the 1D-model we consider the solution domain for $0 \leq x \leq 100 \mu\text{m}$, and in the same way for 2D-model we take a square domain limited by $0 \leq x \leq 100 \mu\text{m}$, and $0 \leq y \leq 100 \mu\text{m}$.

Table 1. Parameter values estimated for Bacterium *P. putida*

Name	Meaning of parameter	Value	Unit
D_U	Diffusion rate of AHL	100	$\mu\text{m}^2/\text{h}$
D_L	Diffusion rate of Lactonase	1	$\mu\text{m}^2/\text{h}$
γ_U	Abiotic degradation rate of AHL	0.005545	1/h
γ_L	Abiotic degradation rate of Lactonase	0.5	1/h
$\gamma_{L \rightarrow U}$	Degradation rate of AHL by Lactonase	$0.65 \cdot 10^9$	1/(mol·h)
α_U	Low production rate of AHL	$1.058 \cdot 10^{-7}$	mol/(1·h)
β_U	Increased production rate of AHL	$1.058 \cdot 10^{-6}$	mol/(1·h)
β_L	Production rate of Lactonase	$1.38 \cdot 10^{-6}$	mol/(1·h)
U_{th}	Threshold of AHL concentration between low and increased activity	$7 \cdot 10^{-8}$	mol/l
ε	Threshold shift for Lactonase production	$5 \cdot 10^{-9}$	mol/l
n	Degree of polymerization	2.5	–
l	Linear size of the object	100	μm

All computations we performed for $N = M = 100$ numbers of nodes over space variables and 100 numbers of nodes over a time variable. This was enough to get a sufficiently accurate solution. To examine the adequacy of the algorithms, we solved test problems with known analytical solutions.

4.1 Dynamics of Components of the Quorum Sensing Model: Numerical Analysis

In the first computational experiment we perform simulations of time-space distributions of the AHL and Lactonase concentrations for 1D model. In this case three bacterial colonies are located at symmetrical positions of the solution domain: $x_c^1 = 0.25l$, $x_c^2 = 0.5l$, $x_c^3 = 0.75l$. The observation time is set after 15 hours. To visualize the dynamics of simulated characteristics we use a time-dependent profile at the central position of $x_c^2 = 0.5l$.

Before considering the results of direct calculations of the AHL and Lactonase concentrations, let us start with the numerical analysis of the contributions of the different parts of the equations, which create the dynamical response of the biological system.

To estimate these contributions, we calculated $U(x_i, t^k)$, $L(x_i, t^k)$ and then evaluated each term in the right sides of PDEs (1), (2) multiplied by the time step $\tau = 0.1$ h. Here we apply the following notations for the equation (1): $P_1 = F_1\tau$ for the source function, $P_2 = D_U\tau U_{xx}$ for the diffusion term, $P_3 = \gamma_U U\tau$ for the AHL degradation term, $P_4 = \gamma_{L \rightarrow U} L U\tau$ for the term specified the degradation of AHL by Lactonase. In the same way for the equation (2) we have: $Q_1 = F_2\tau$ for the source function, $Q_2 = D_L\tau L_{xx}$ for the diffusion term, $Q_3 = \gamma_L U\tau$ for the Lactonase degradation term.

Figure 3 shows the contributions of the different parts of the equation (1) defined dynamics of the AHL concentration as time-dependent functions. The dynamics of the model components for the Lactonase concentration is illustrated in Fig. 4.

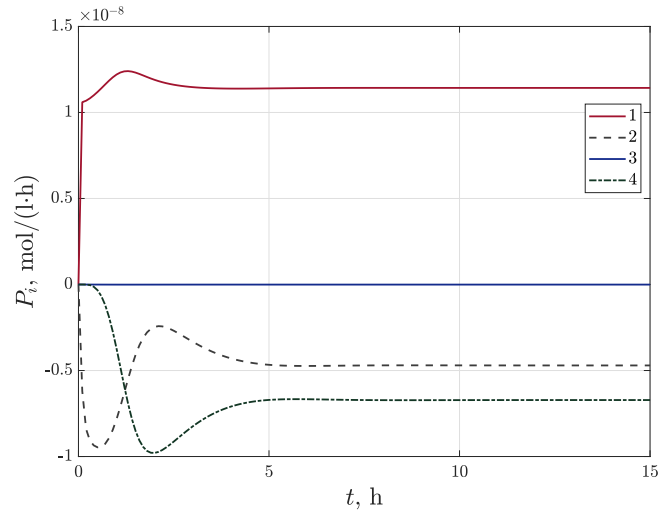


Fig. 3. The time-dependent parts of right side corresponding to the equation (1) defined the AHL concentration dynamics: $P_1(t) - 1$, $P_2(t) - 2$, $P_3(t) - 3$, $P_4(t) - 4$.

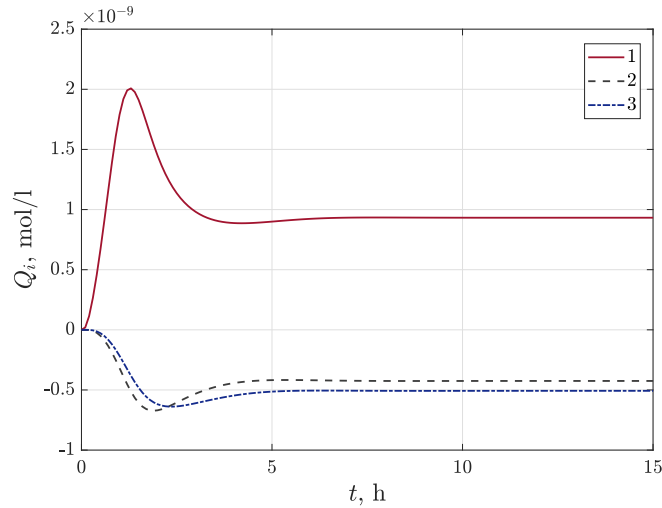


Fig. 4. The time-dependent parts of the right hand side corresponding to the equation (2) defined the Lactonase concentration dynamics: $Q_1(t) - 1$, $Q_2(t) - 2$, $Q_3(t) - 3$.

These graphs allow us to see which processes a priority affect the distributions of the AHL and Lactonase concentrations for given parameter values. Here we can conclude, that the AHL own degradation $P_3(t)$ specified by the term of $\gamma_U U \tau$ has a negligible influence on the resulting AHL distribution. Indeed, this degra-

dation is very small under realistic conditions. At the initial time moments, the dynamics of the AHL concentration is determined mainly by the production term and diffusion process followed by the influence of the Lactonase. The changes in the Lactonase concentration are determined by production, diffusion and the own degradation simultaneously during the whole time range. It is obvious that after 6-7 hours the state of the biological system tends to relaxation in general. These effects are observed under natural conditions with self-produced AHL and Lactonase. Hence we may assume that a variation of external exposure can result in changes in a state of the biological system. In particular, the artificial supply can lead to relevant changes in the AHL and Lactonase concentrations. This potentially means that we can artificially influence the quorum sensing of a bacterial population.

4.2 Simulation of Quorum Sensing Characteristics under Changes of External Conditions

In this Section we present the results of numerical simulation of bacterial quorum sensing under variation of external exposure. Specifically, we consider the artificial addition of the AHL and Lactonase at certain time point t^* . Here we also consider the implementation of the one-dimensional model for three bacterial colonies located at fixed positions. The observation time is set to be 15 hour. The simulated characteristics are visualized at the central position $x_c^2 = 0.5l$. Figures 5 and 6 show the time-dependent profiles of the AHL and Lactonase concentrations under variations of external conditions.

Here we consider four modes: without any influence, under the addition of the external AHL concentration 9.9 nmol/l equal to the value of the own AHL concentration at the time moment $t^* = 6$ h, under the addition of the external Lactonase concentration 8.03 nmol/l equal to the current value of Lactonase at the time moment $t^* = 6$ h, and under the addition both of them. These data suggest that the addition of the external AHL concentration leads to a rapid rise not only in the AHL but also in the Lactonase concentration. This is followed by the AHL concentration (with respect to natural conditions) due to the presence of the negative feedback. These basic findings are consistent with research [9] showing that slight fluctuations of signaling compounds arise under supplying the external AHL, that can be visualized with the use of inverted microscopy.

At the same time the external addition of the Lactonase causes a significant decrease in the concentration of signaling molecules. Furthermore, the addition both of substances gives rise to an increase in the AHL concentration before falling to certain value. The example of time-spatial visualization of the computed AHL and Lactonase concentrations are shown in Fig. 7 and Fig. 8. The simulation time equals 30 hours. During the period from hour 6 to hour 12, every two hours the external concentration of Lactonase enzymes 32 nmol/l was added. This yields that the AHL concentration drops dramatically to approximately 1.5 nmol/l.

Since the AHL concentration is referred to as the quorum sensing “level”, we can make bacteria “fall silent” during the period of action of the external

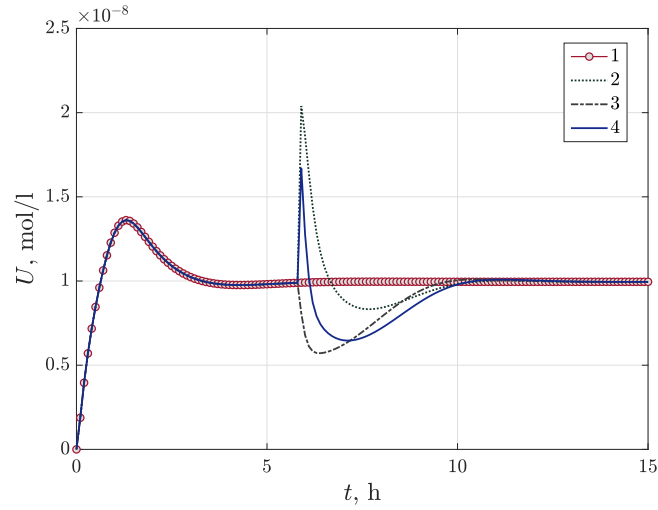


Fig. 5. The time-dependent profiles of the AHL concentration at $t^* = 6$ h under the conditions: 1 – without impact, 2 – at the addition of the external AHL, 3 – at the addition of the Lactonase, 4 – at the addition both of AHL and Lactonase.

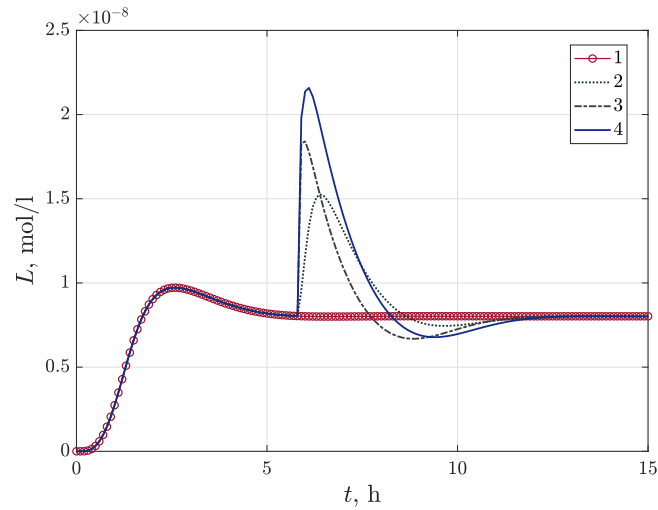


Fig. 6. The time-dependent profiles of the Lactonase concentration at $t^* = 6$ h under the conditions: 1 – without impact, 2 – at the addition of the external AHL, 3 – at the addition of the Lactonase, 4 – at the addition both of AHL and Lactonase.

Lactonase concentration. This implies that this period can be used to apply antibiotic treatment for some pathogen bacterial strains, which demonstrate high

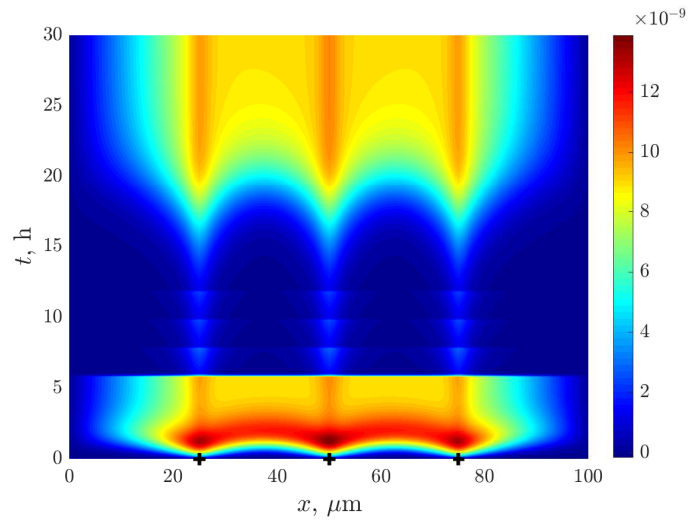


Fig. 7. The time-spatial distribution of the AHL concentration under the external addition of the Lactonase enzymes.

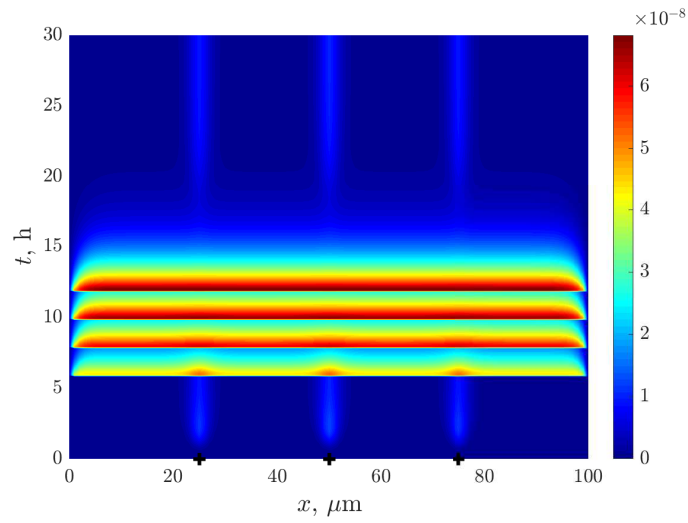


Fig. 8. The time-spatial distribution of the Lactonase concentration under the external addition of Lactonase.

tolerance to antibiotics due to quorum sensing. For example *P. putida* strains exhibit resistance to a large number of antibiotics [10]. The developed reaction-diffusion model can potentially help to estimate the dose of external substances

needed to be added to control bacterial quorum sensing and the optimal time points for these additions.

4.3 2D Simulation of Quorum Sensing Characteristics

The computer simulation based on the 2D-model allows us to visualize the quorum sensing characteristics in more realistic manner. In this case we will present the simulation results for the 2D reaction-diffusion model combined with the procedure of the Monte-Carlo simulation of bacterial population growth. According to above algorithm, one, two or three bacterial colonies with a circle shape can start to grow at initial time moment. The radius of each bacterial colony is set to be $1 \mu\text{m}$. Simulation results are presented in Fig. 9.

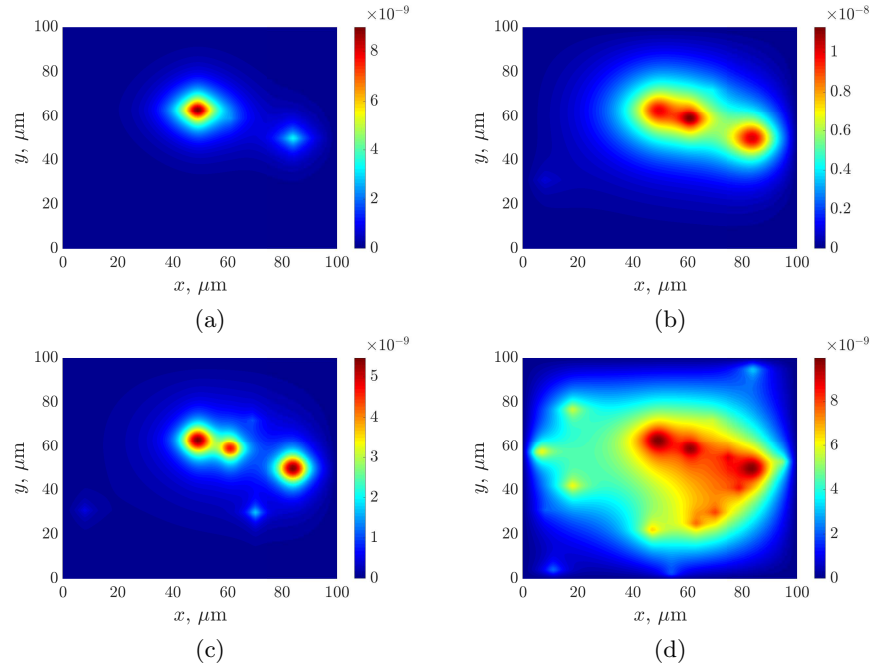


Fig. 9. The dynamics of AHL space distribution at the fixed time moments: (a) $t = 3$ h; (b) $t = 7.25$ h; (c) $t = 7.75$ h; (d) $t = 25$ h.

The total simulation time corresponds to 25 hours. During this period bacterial colonies are growing. If the total size of all bacterial colonies reaches the value of $R_0 = 20 \mu\text{m}$, the growth finishes due to the underlying model assumption while new small colonies still can appear. One limitation of our implementation is that only the stage of bacterial growth is under consideration (in reality the degradation phase is followed by the growth phase). Here we assume that at the

time point $t^* = 7.5$ h, when the total linear size reaches R_0 , the external Lactonase concentration of $0.5 \cdot 10^{-8}$ mol/l is added artificially. There are eighteen bacterial colonies simulated with logistic-stochastic procedure during this computational experiment. Figure 9 shows four frames with spatial distributions of the AHL concentration calculated at the time moments: $t = 3$ h corresponding the stage of bacterial growth under natural conditions (Fig. 9 (a)), $t = 7.25$ h – before 0.25 h the addition of the external Lactonase enzymes (Fig. 9 (b)), $t = 7.75$ h – after 0.25 h from the addition of Lactonase (Fig. 9 (c)) and $t = 25$ h – at the end of the simulation process (Fig. 9 (d)).

The graph in Fig. 10 demonstrates the dynamics of changes in the maximum value of the Lactonase concentration of the whole biological system. As it can be expected that even a single injection of the external Lactonase leads to a significant decrease of the AHL concentration. The maximum value of the AHL concentration falls to the level of 5 nmol/l and then starts again to grow due to mechanisms which underline the mathematical model.

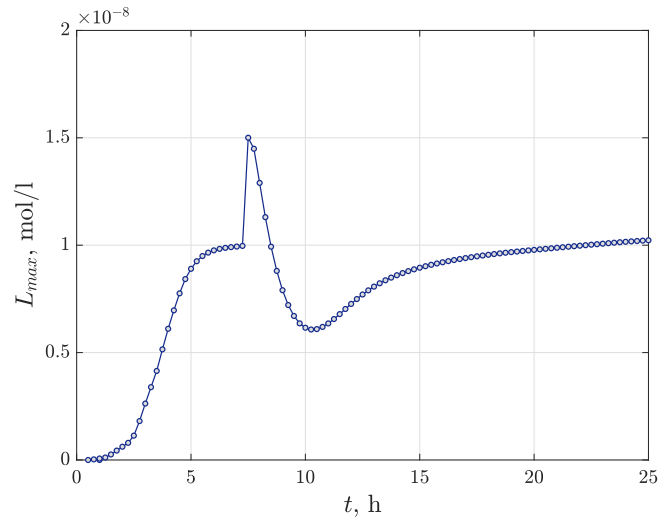


Fig. 10. The time-dependent profile of maximum values of the Lactonase concentration calculated during the simulation.

These findings suggest that artificial supply to bacterial populations by an additional enzyme permits to influence the process of bacterial communication significantly. For example, the external addition of Lactonase allows one to perform an antibacterial treatment in the sense of reducing, e.g., their pathogenicity. Thus, the reaction-diffusion model of bacterial quorum sensing can be potentially used as a scientific support for processes to control the population-communication of bacteria.

5 Conclusion

In summary, this paper suggests a modification of the reaction-diffusion model of bacterial quorum sensing based on combination of the deterministic approach with logistic-stochastic simulation procedure of bacterial population dynamics.

For the numerical computer implementation of 1D as well as 2D models we proposed computational schemes based on a joint application of finite difference methods and iterative procedures. This allows to provide the accuracy corresponding to the order of approximation of applied numerical methods for solving semilinear reaction-diffusion equations. The computational schemes have second order accuracy with respect to space and time variables and are absolutely stable. To describe the dynamics of bacterial colonies we also proposed the algorithm based on Monte-Carlo simulation. The algorithm includes the scheme of logistic growth of bacterial colonies.

The general computational schemes both for 1D model and 2D model were implemented using Matlab programming. A designed application software was applied for computer simulations of time-dependent characteristics of bacterial cooperative behaviour.

We conducted a series of computational experiments specifically for *Pseudomonas putida* bacterial strains, for which the quorum sensing phenomenon and producing a special enzyme, the Lactonase, are well studied in biological experiments and corresponding mathematical models.

The computer simulated time-space distributions of the AHL and Lactonase concentrations are presented with a focus on their changes under the external addition of substances. Our findings indicate that the repeated addition of Lactonase enzymes can significantly reduce the AHL concentration. As far as the AHL concentration is associated with the quorum sensing “level”, we can make bacteria “fall silent” during the period of action of the external Lactonase concentration. This effect allows to make the application of antibiotic treatment more effective for some pathogenic bacterial strains. Therefore, the developed model of bacterial quorum sensing might be addressed in future studies of predicting and controlling population-communication of bacteria, where spatial heterogeneity plays a relevant role.

References

1. Ananda, M., Rusmana, I., Akhdiya, A.: Quorum quenching of *Bacillus cereus* INT1c against *Pseudomonas syringae*. IOP Conf. Series: Journal of Physics: Conf. Series **1277**, 012010(9) (2019)
2. Dockery, J.D., Keener, J.P.: A mathematical model for quorum sensing in *Pseudomonas aeruginosa*. Bull. Math. Biol. **63**, 95–116 (2001)
3. Fekete, A., Kuttler, C., Rothballer, M., Hense, B.A., Fischer, D., Buddrus-Schiemann, K., Lucio, M., Müller, J., Schmitt-Koppling, P., Hartmann, A.: Dynamic regulation of N-acyl-homoserine lactone production and degradation in *Pseudomonas putida* *IsoF*. FEMS Microbiol. Ecol. **72**, 22–34 (2010)

4. Kalia, V.C. (ed): Quorum sensing vs quorum quenching: a battle with no end in sight. Springer, India (2015)
5. Kovtanyuk, A.E., Chebotarev, A.Yu., Botkin, N.D., Turova, V.L., Sidorenko, I.N., Lampe, R.: Continuum model of oxygen transport in brain. *J. Math. Anal. Appl.* **474**, 1352–1363 (2019)
6. Kovtanyuk, A.E., Chebotarev, A.Yu., Botkin, N.D., Turova, V.L., Sidorenko, I.N., Lampe, R.: Nonstationary model of oxygen transport in brain tissue. *Comp. Math. Meth. Med.* **2020**, 4861654 (2020)
7. Kuttler, C.: Reaction-diffusion equations and their application on bacterial communication. *Handbook of statistics (Chapter 4)*, 55–91 (2017)
8. Maslovskaya, A.G., Moroz, L.I., Chebotarev, A.Yu., Kovtanyuk, A.E.: Theoretical and numerical analysis of the Landau–Khalatnikov model of ferroelectric hysteresis. *Commun. Nonlin. Sci. Num. Simulat.* **93**, 105524 (2020)
9. Meyer, A., Megerle, J.A., Kuttler C., Müller, J., Aguilar, C., Eberl, L., Hense, B.A., Rädler, J.O.: Dynamic of AHL mediated quorum sensing under flow and non-flow conditions. *Phys. Biol.* **9**, 026007(10) (2012)
10. Molina, L., Udaondo, Z., Duque, E., Fernández, M., Molina-Santiago, C., Roca, A., Porcel, M., de la Torre, J., Segura, A., Plesiat, P., Jeannot, K., Ramos, J.L.: Antibiotic resistance determinants in a *Pseudomonas putida* strain isolated from a hospital. *PloS one* **9**(1), e81604 (2014)
11. Müller, J., Kuttler, C., Hense, B.A., Rothballer, M., Hartmann, A.: Cell-cell communication by quorum sensing and dimension-reduction. *J. Math. Biol.* **53**, 672–702 (2006)
12. Pang, Z., Raudonis, R., Glick, B.R., Lin, T.-J., Cheng, Z.: Antibiotic resistance in *Pseudomonas aeruginosa*: mechanisms and alternative therapeutic strategies. *Biotechnology Advances* **37**(1), 177–192 (2019)
13. Perez-Velazquez, J., Gölgeli, M., Garcia-Contreras, R.: Mathematical modelling of bacterial quorum sensing: a review. *Bull. Math. Biol.* **76**, 1585–1639 (2016)
14. Roberts, P.A., Huebinger, R.M., Keen, E., Krachler, A.-M., Jabbari, S.: Mathematical model predicts anti-adhesion antibiotic debridement combination therapies can clear an antibiotic resistant infection. *PLoS Comput. Biol.* **15**(7), e1007211(39) (2019)
15. Samarskii, A.A.: The theory of difference schemes. Marcel Dekker Inc., New York (2001).
16. Whitehead, N.A., Barnard, A.M.L., Slater, H., Simpson, N.J.L., Salmond, G.P.C.: Quorum sensing in Gram-negative bacteria. *FEMS Microbiol. Rev.* **25**, 365–404 (2001)
17. Williams, P., Winzer, K., Chan, W.C., Camara, M.: Look who’s talking: communication and quorum sensing in the bacterial world. *Phil. Trans. R. Soc. B.* **362**, 1119–1134 (2007)
18. Zhao, X., Yu, Z., Ding, T.: Quorum-sensing regulation of antimicrobial resistance in bacteria. *Microorganisms* **8**(3), 425–446 (2020)